

Towards An Autonomous sUAS Operating in UTM TCL4+ and STEReO Fire Scenario

Joshua Baculi* & Corey Ippolito†

NASA Ames Research Center, Moffett Field, CA 94035

This study presents two sUAS payload point designs for enabling autonomous BVLOS flight in UTM TCL4+ urban environments and STEReO fire responses. The payload components for the first payload include an onboard computer and a 360° LIDAR. The second payload, which is a continuation of the first, adds a range finder altimeter, downward-facing monocular camera, forward-facing thermal and visible light dual camera, vehicle-to-vehicle radio modem, and Li-ion smart battery. The components are mounted on enclosed structural frames that were designed in-house. Placing the autonomy components onboard leverages the advantages of sUAS over manned aircraft such as low-cost, quick response time, and increased scalability. Autonomous capabilities include embedded processing, SLAM, object and fire detection, and V2V communication. Data processing is conducted onboard the aircraft to eliminate the dependency on a groundstation downlink. The first iteration of the payload is tested in both simulation and flight tests while the continuing iteration is in development.

I. Introduction

IN order for unmanned aerial vehicles (UAVs) to operate in more complex flight environments, the vehicle autonomy components—processing, localization, sensing, communication—must be capable of ensuring the safety of the vehicle, persons, and environment. For example, flying in urban settings presents both known hazards and uncertainties.¹ An a priori map may be available to create a trajectory around buildings, but changing wind fields, moving crowds of people below the flight path, and spotty communication and navigation are difficult to completely predict pre-flight.

To safely allocate airspace for unmanned aircraft systems (UAS), NASA’s UAS Traffic Management (UTM)² system categorized its development into four Technical Capability Levels (TCL),³ with each subsequent TCL increasing in complexity and density. The first level, TCL1, covers the simplest airspace over unpopulated land or water with pilot control and little manned aviation traffic. Our aircraft participated in the TCL4+ phase where beyond visual line-of-sight (BVLOS) flight in higher density urban environments requires some level of autonomy.

In addition to TCL4+, our aircraft participates in the Scalable Traffic Management Emergency Response Operations (STEReO) project, which is an extension of UTM for UAS flight where a temporary flight restriction (TFR) may be in place due to an emergency such as a wildfire or hurricane. Currently focusing on wildfire efforts, our sUAS’ goals in STEReO include improving disaster response time, enabling large-scale operations, improving operator awareness, and demonstrating safety and resiliency in these operations.⁴ The adverse conditions inherent to emergency response scenarios can be handled by a robust platform that is adaptable to a variety of contingencies.

A. Contribution

The small UAS (sUAS) presented in this study carries a payload that enables fully autonomous flight with no operator control required as all of the autonomy components are handled onboard. Two iterations of this payload have been developed for the sUAS. Much of the first payload, called the Gen 2.1 payload, has been

*Systems Engineer, HX5, LLC., NASA Ames Research Center, Moffett Field, CA 94035, AIAA Member.

†Aerospace Scientist, NASA Ames Research Center, Moffett Field, CA 94035, AIAA Member.

developed over the years as part of the Safe Autonomous Flight Environment (SAFE50) project¹ project that focuses on autonomous sUAS operating below 50 ft in urban environments. The Gen 2.1 payload is a continuation of a previously designed payload that includes an onboard 360° LIDAR to handle localization in GPS-degraded environments⁵ such as urban canyons or hilly forests and an onboard computer running Linux for real-time data processing. The onboard computer runs the NASA in-house Reflection Architecture.⁶ Through Reflection, the sUAS is able to perform LIDAR SLAM, local and global path planning,⁷ decision-making,⁸ air and ground communication, and object detection. The Gen 2.1 payload has been tested in simulation, ground, and flight tests that demonstrate the integration of onboard autonomy components.

The second payload, called the Gen 3 payload, also includes a 360° LIDAR and Linux onboard computer, and adds several new autonomy components. A radio vehicle-to-vehicle (V2V) communication protocol⁹ is employed for cooperative collision avoidance and local path planning.¹⁰ A dual thermal and visible light camera detects human heat signatures for dynamic ground risk mitigation¹¹ and fire edge detection. The individual components of the Gen 3 payload have been tested in simulation and hardware in the loop tests. The overall payload is currently in the hardware integration stage of development. It is important to note that the payloads serve as point designs to enable autonomous operations and the hardware selected may not necessarily be the optimal components.

II. Airframe

The Gen 2.1 and 3 payloads are designed to be mounted on the DJI Matrice 600 (M600) Pro shown in Figure 1. Per the aircraft specs in Table 1, the M600 Pro is a hexacopter capable of hovering for 18 minutes with a 5.5 kg max payload.¹² The DJI A3 Pro autopilot includes three IMUs and three GPS receivers for redundancy. In the event one GPS loses signal, another GPS takes over. The aircraft is controllable through DJI's proprietary iOS applications. The apps are run on an iPad connected to a remote controller (RC) that communicates directly to the aircraft. Through these apps, the aircraft is capable of manual and waypoint flight. When flying waypoints, the pilot may take manual control at any point.



Figure 1: Gen 2.1 payload mounted on the M600 Pro.

The payloads are mounted via the payload mounting rack included on the M600 Pro. Figure 2 shows a prototype of the Gen 2.1 payload mounted on the uninstalled M600 Pro payload mounting rack. The payload rack is comprised of 12 mm diameter carbon fiber bars that are attached to the frame of the aircraft. The versatile design allows a variety of payloads to be mounted by simply clamping directly to the bars. The Gen

Table 1: DJI M600 Pro specifications.¹²

Aircraft	DJI M600 Pro
Configuration	Hexacopter
Weight	10 kg (TB48S batteries)
Max Takeoff Weight	15.5 kg
Flight Duration	38 min hovering (no payload); 18 min hovering (max payload)
Range	5 km unobstructed FCC transmission compliant
Max Speed	65 kph
Max Altitude	2,500 m ASL (2170R propellers); 4,500 m ASL (2195 propellers)
Max Wind Speed	8 m/s
Operating Temperature	-10–40 °C
Payload Capacity	5.5 kg
Autopilot	DJI A3 Pro
Data Links	2.400 to 2.483 GHz; 5.725 to 5.825 GHz
Power System	Six (6) TB48S LiPo batteries (5700 mAh 6S 22.8 V)

2.1 payload shown in Figure 2 is slid onto the payload rack so that the LIDAR is aligned with the vertical axis of the aircraft before tightening in place. By enabling payloads to be positioned along the front-to-back axis, the payload center of gravity (CG) can be better aligned with the aircraft CG to improve stability.

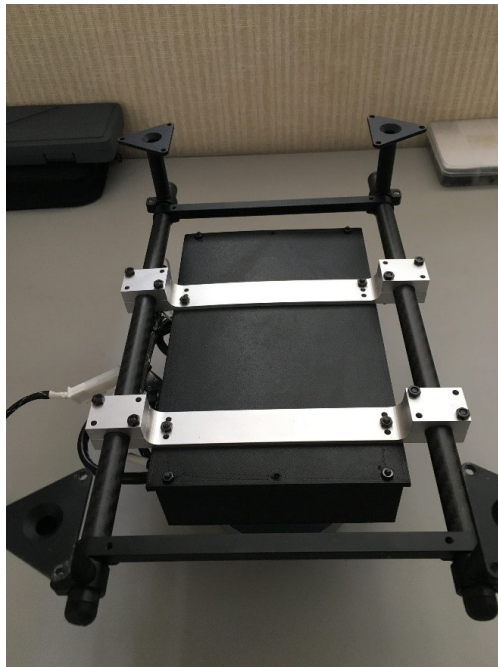


Figure 2: The Gen 2.1 payload's aluminum rails (silver) clamp onto the M600 Pro payload rack (round carbon fiber bars).

III. Payloads

A. Gen 2.1 Payload

The Gen 2.1 payload shown in Figure 3 is a modification of a payload previously flown on a DJI S1000 octocopter.⁵ That payload included an onboard computer running Ubuntu, 360° LIDAR, voltage regulator, and IMU. The Gen 2.1 payload modified the mounting rails to fit the M600 Pro and added a LiPo battery, circuit breaker, and 3D printed enclosures. The onboard computer handles all of the autonomy processing through Reflection, an embedded autonomy architecture developed at NASA Ames.⁶ Autonomy functions include SLAM from the LIDAR and communication to the DJI A3 Pro autopilot by receiving telemetry information and in turn sending velocity commands. Figure 4 shows the Gen 2.1 component connections, including data and power. The IMU of the previous payload is left on the Gen 2.1, but is unused due to the M600 Pro having three redundant IMUs built into the DJI A3 Pro. The A3 Pro connection does not require power since the autopilot is powered by the aircraft batteries along with the other avionics. The circuit breaker connects the battery to the voltage regulator, which then sends power to the LIDAR and onboard computer. The separate battery allows the payload to be powered separately from the aircraft, with the only electrical connection between payload and aircraft being the data connection between the autopilot and the onboard computer.



Figure 3: Fully enclosed Gen 2.1 payload mounted on the M600 Pro.

The payload is held together by several aluminum structural component that secure the LIDAR, onboard computer, voltage regulator, and IMU into a single unit. This unit is then mounted to the aluminum mounting rails that mount to the M600 Pro payload rack. An acrylic plate is placed between the rails and the unit to enclose the top of the payload and to carry the LiPo battery and enclosures. The enclosures are 3D printed to cover the unit and circuit breaker such that the LIDAR FOV is unobstructed while allowing cables to be plugged into the onboard computer and the circuit breaker button to be pressed.

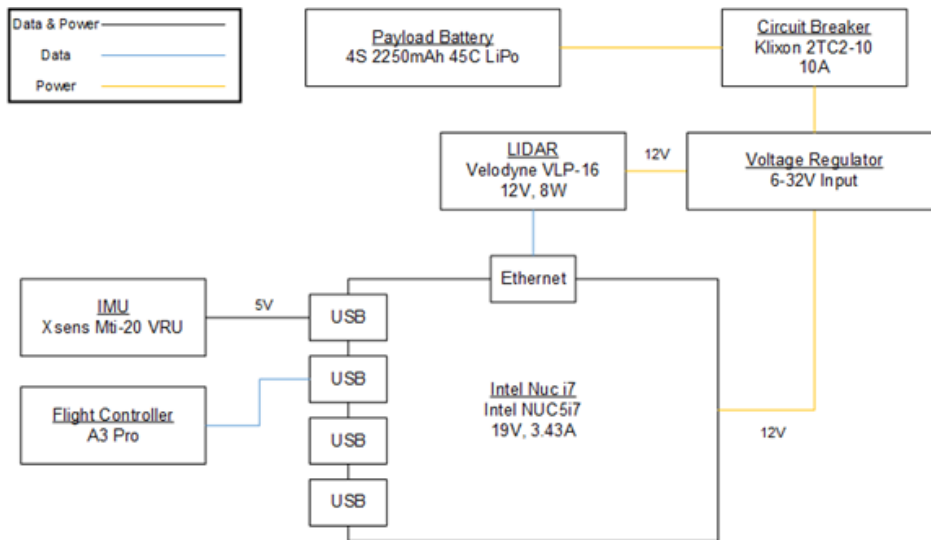


Figure 4: Gen 2.1 payload block diagram showing data and power connections.

1. Gen 2.1—Electrical Analysis

Table 2 shows the electrical analysis based on the rated power requirements of the Gen 2.1 payload autonomy components. From the specs provided by the component data sheets, the payload is expected to operate at 53.00 W when all of the components are nominally functioning and at 101.17 W at max output. Based on the regulator specified 12 V output and 10 A peak current, Table 2 shows even max operation yields a sufficient margin of safety of 0.19. Figure 5 shows the Gen 2.1 payload consuming 52.9 W while running LIDAR SLAM. This matches the expected nominal operation power consumption shown in Table 2.

Table 2: Gen 2.1 payload power sizing calculations. “Reg:” indicates voltage regulator specification/calculation.

	Nominal Operation	Max Operation
Total Power (W)	53.00	101.17
Reg: Efficiency	97.00%	97.00%
Reg: Efficiency Power Loss (W)	1.59	3.04
Reg: Programmed Output Voltage (V)	12.00	12.00
Reg: Output Current (A)	4.42	8.43
Reg: Max Output Current (A)	8.00	10.00
Factor of Safety, actual/max	1.81	1.19
Margin of Safety, $FoS - 1$	0.81	0.19

Tables 3 and 4 show the calculated requirements for the payload battery and voltage regulator, respectively. The 12 V desired regulator output voltage used in Table 2 is also used in these calculations. Tables 3 and 4 show that the battery and regulator should be capable of outputting 9.27 A for a 1.10 factor of safety. In addition to the 10 A fuse on the voltage regulator, the electrical system is supplemented with a 10 A circuit breaker. This redundancy further safeguards the payload’s electrical components.

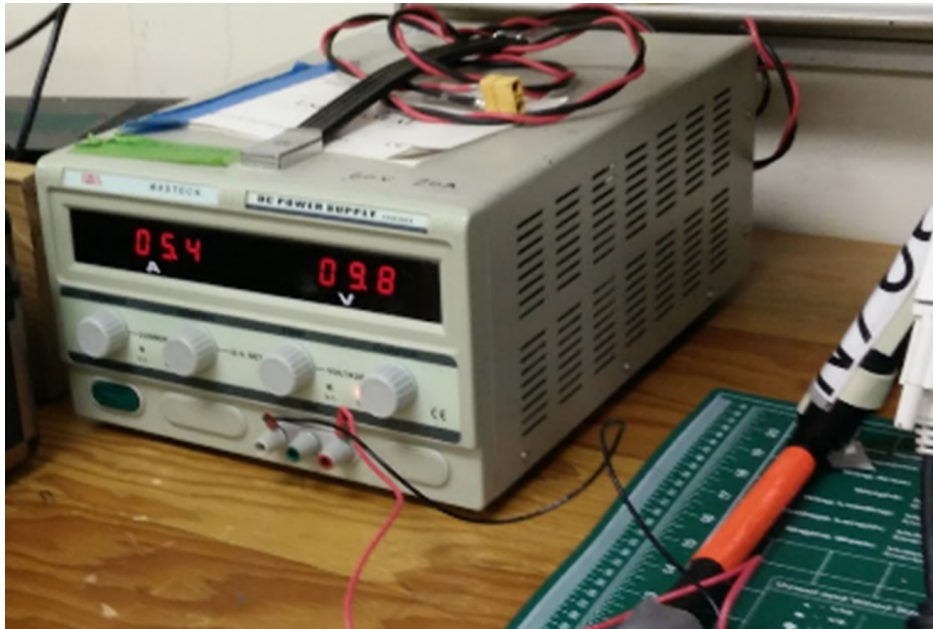


Figure 5: Gen 2.1 payload power consumption test while running LIDAR SLAM. At 9.8 V, the Gen 2.1 payload drew 5.4 A, resulting in 52.9 W power consumption.

Table 3: Gen 2.1 payload battery sensor sizing and requirements.

	Nominal Operation	Max Operation
Total System Power (W)	53.00	101.17
Voltage (V)	14.80	12.00
Current (A)	3.58	8.43
Desired FoS		1.10
Required Current (A)		9.27

Table 4: Gen 2.1 payload regulator sizing and requirements.

	Nominal Operation	Max Operation
Reg: Power (W)	53.00	101.17
Reg: Voltage Output (VDC)	12.00	12.00
Reg: Current (A)	4.42	8.43
FoS		1.10
Regulator Current Output (A)		9.27

2. Gen 2.1—Mechanical Analysis

The Gen 2.1 payload consisting of the onboard computer, LIDAR, IMU, voltage regulator, battery, circuit breaker, structural rails, and enclosures as well as all of the wiring and fasteners has an estimated mass of ~ 1700 g. This is well below the 5500 g max payload mass limit shown in Table 1 and Table 5 shows that the payload mass has a more than adequate 2.24 margin of safety.

The two main structural components of the Gen 2.1 payload are the mounting rail and clamp that secure the payload to the M600 Pro. These two components were CNC machined out of 7075-T6 aluminum. Figure 6 shows the mounting rail stress analysis conducted using Solidworks SimulationXpress. To calculate the

Table 5: Gen 2.1 payload mass calculations. The payload mass was estimated by subtracting the payload-less aircraft mass from the payload-mounted aircraft.

Estimated Payload Mass (g)	~1700
Aircraft Max Payload Mass (g)	5500
Factor of Safety, actual/mass	3.24
Margin of Safety, $FoS - 1$	2.24

stresses, a max 5500 g payload is assumed to be undergoing a 5 G maneuver: $5.5 \text{ kg} \times 5 \text{ G} \times 9.8 \text{ m/s} = 269.5 \text{ N}$. This applied load is intended to be a worst case scenario where the mounting rail is pushed to its carrying limit. The stress analysis fixes the mounting rail at the fastener holes that connect to the clamp. Because there are two mounting rails and two mounting points for each rail, the load applied to each payload mounting point is 67.37 N. Solidworks SimulationXpress stresses the parts by slowly applying static loads and calculating the von Mises stress profile from there. The minimum factor of safety for the mounting rail under these conditions is 33. Therefore, the mounting rail is more than durable enough for the M600 Pro's max allowable payload. Furthermore, all components are secured with locknuts and supplemented with threadlocker.

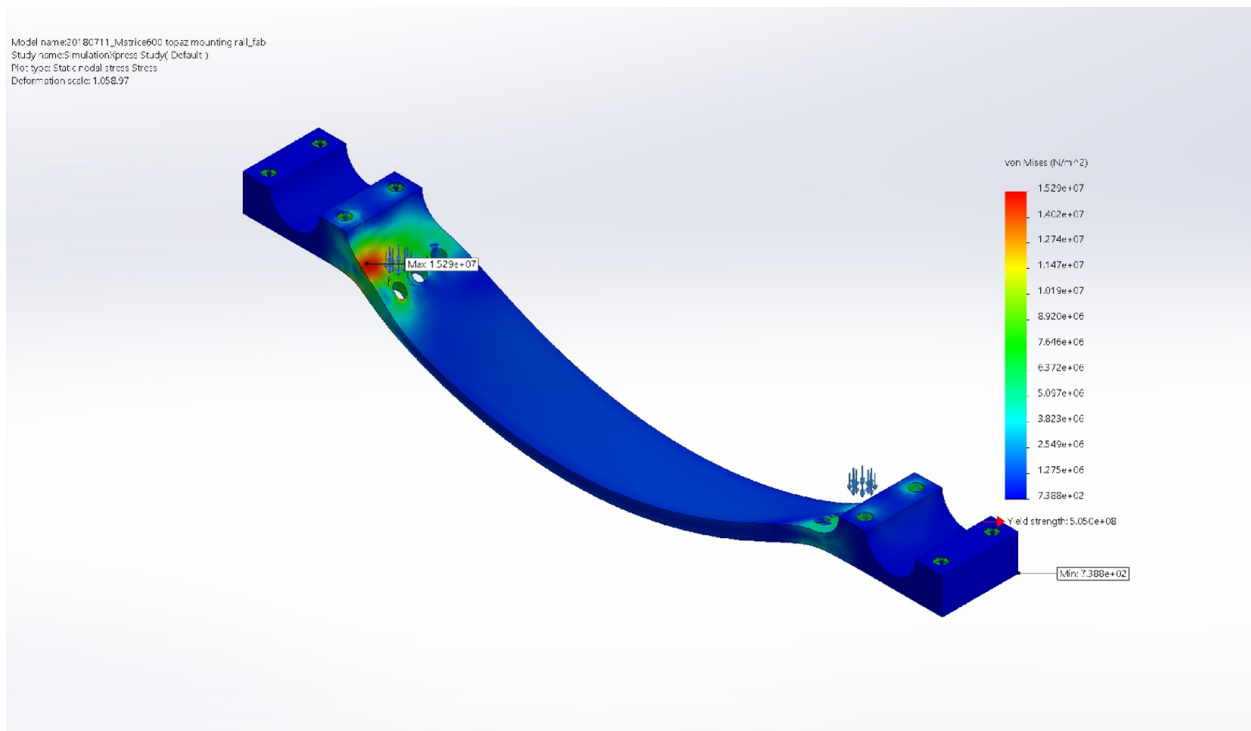


Figure 6: Mounting rail von Mises stress profile conducted in Solidworks. The fixtures are at the fastener holes connecting the rail to the clamp. The load is applied around the fastener holes where the payload is mounted. 67.37 N are applied at each load point. The minimum factor of safety is 33.

B. Gen 3 Payload

Figure 7 shows the CAD model of the Gen 3 payload. The Gen 3 payload keeps the same circuit breaker and LIDAR model as the Gen 2.1 and upgrades to a newer onboard computer model and a higher spec'ed voltage regulator. The onboard computer still runs the Ubuntu operating system. In addition to the components already present in the Gen 2.1 payload, the Gen 3 payload adds the following components:

- Range finder altimeter

- Downward-facing monocular camera
- Forward-facing visible light and thermal camera
- V2V radio modem
- Smart battery

Through Reflection, the onboard computer processes SLAM from the LIDAR, above ground level (AGL) altitude from the altimeter, fire and object detection from the dual and monocular cameras, communication from the radio modem, and power measurements from the smart battery.

The payload is held together by several structural components:

- Aluminum battery plate
- Aluminum bottom plate
- Four aluminum bracket clamps
- Four vibration-damping sandwich mounts
- Eight hex aluminum standoffs

The battery and bottom plates were cut to size from 2 mm 6061 aluminum plates. Component mounting holes were precisely drilled using a 2.5D CNC mill. The aluminum bracket clamps were CNC machined from 6061 aluminum and connect the battery plate to the aircraft payload rack. Each bracket clamp connects to the battery plate through a vibration-damping sandwich mount intended to mitigate the effect of aircraft vibration on the cameras. The hex standoffs connect the battery and bottom plates to make a box-like frame for the payload. Finally, the box frame is enclosed with transparent acrylic panel walls to allow the interior components to be inspected pre-flight while still protecting the interior during flight.

Components that need unobstructed fields of view (FOV) such as the cameras and LIDAR are either mounted outside of the enclosed box frame or are mounted so that the FOV lies outside the box. Because the battery and circuit breaker are frequently interacted with (e.g. replacing the battery, opening/closing the circuit breaker), they are also mounted outside of the enclosed box on top of the battery plate.

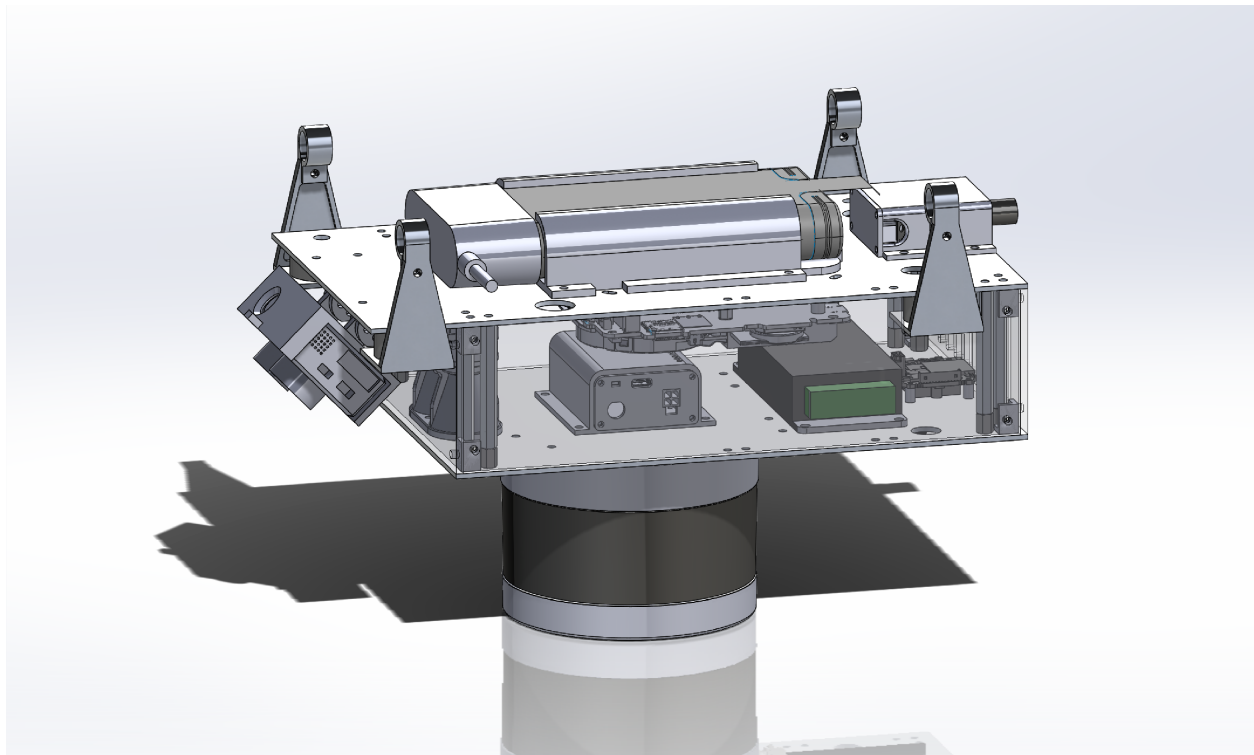


Figure 7: Gen 3 payload CAD model.

The block diagram in Figure 8 shows the data and power connections throughout the Gen 3 payload. The onboard computer, LIDAR, and V2V modem are powered directly by the smart battery through the voltage regulator, whereas the two cameras and range finder receive power from the onboard computer via

USB. The A3 Pro is powered separately by the aircraft batteries and only connects to the Gen 3 payload for data.

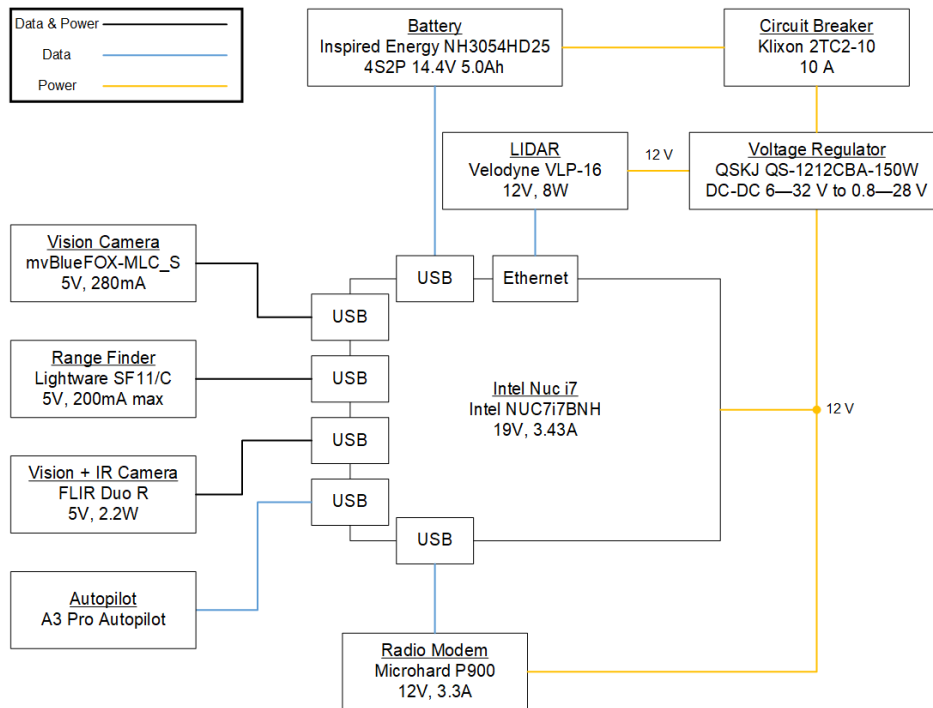


Figure 8: Gen 3 payload block diagram showing data and power connections.

1. Gen 3—Electrical Analysis

Table 6 shows the Gen 3 payload electrical analysis. Per the component specifications, the Gen 3 payload is expected to operate at 60.90 W nominally and at 112.70 W max. Based on a 12 V regulator output and 15 A max current, Table 6 shows a sufficient 0.6 margin of safety at max operation.

Table 6: Gen 3 power sizing calculations. “Reg:” indicates voltage regulator specification/calculation.

	Nominal Operation	Max Operation
Total Power (W)	60.90	112.7
Reg: Efficiency	97.00%	97.00%
Reg: Efficiency Power Loss (W)	1.83	3.38
Reg: Programmed Output Voltage (V)	12.00	12.00
Reg: Output Current (A)	5.08	9.39
Reg: Max Output Current (A)	15.00	15.00
Factor of Safety, actual/max	2.96	1.60
Margin of Safety, $FoS - 1$	1.96	0.60

Tables 7 and 8 uses the 12 V desired regulator output voltage from Table 6 to calculate the requirements for the payload battery and voltage regulator, respectively. Tables 7 and 8 show that the battery and regulator should be capable of outputting 10.30 A for a 1.10 factor of safety.

Table 7: Gen 3 battery sensor sizing and requirements.

	Nominal Operation	Max Operation
Total System Power (W)	60.90	112.70
Voltage (V)	14.80	12.00
Current (A)	4.10	9.39
Desired <i>FoS</i>		1.10
Required Current (A)		10.30

Table 8: Gen 3 regulator sizing and requirements.

	Nominal Operation	Max Operation
Reg: Power (W)	60.90	112.70
Reg: Voltage Output (VDC)	12.00	12.00
Reg: Current (A)	5.08	9.39
FoS		1.10
Regulator Current Output (A)		10.30

2. Gen 3—Mechanical Analysis

As previously stated, the structural frame of the payload consists of two 6061 aluminum plates and eight 6 mm hex aluminum standoffs. Figure 9 shows the physical structure of the payload with most of the components mounted. Also shown are the bracket clamps that connect the top battery plate to the M600 Pro payload rack. The bracket clamps connect to the battery plate via vibration damping sandwich mounts to mitigate the aircraft vibration effects on the payload sensors. All fasteners are 316 stainless steel and are fixed using nylon-insert stainless steel locknuts and washers. At the time of this paper, Figure 9 shows the latest status of the Gen 3 payload. Wiring between and properly fastening the components remains to be completed. As such, mass measurements and power tests have not been taken.

Figure 10 shows the Solidworks SimulationXpress stress analysis on the bracket clamp. The part is fixed at the inner face that clamps around the payload rack and the load is applied downwards onto the surface where the vibration damper is fastened. The same 269.5 N load from Section III.A.2 is applied. Because there are four bracket clamps per payload, 67.38 N is applied. The resulting analysis yields a minimum factor of safety of 3.17, well above the 1.1 minimum requirement. Figure 11 shows the stress analysis applied to the Gen 3 payload structural frame. The structural frame is fixed around the vibration mounts that connect to bracket clamp. The full 269.5 N load is applied to the front face of the bottom plate to simulate the highest amount of stress the frame might feel. These testing conditions result in a 1.38 minimum factor of safety, also above the 1.1 minimum requirement.

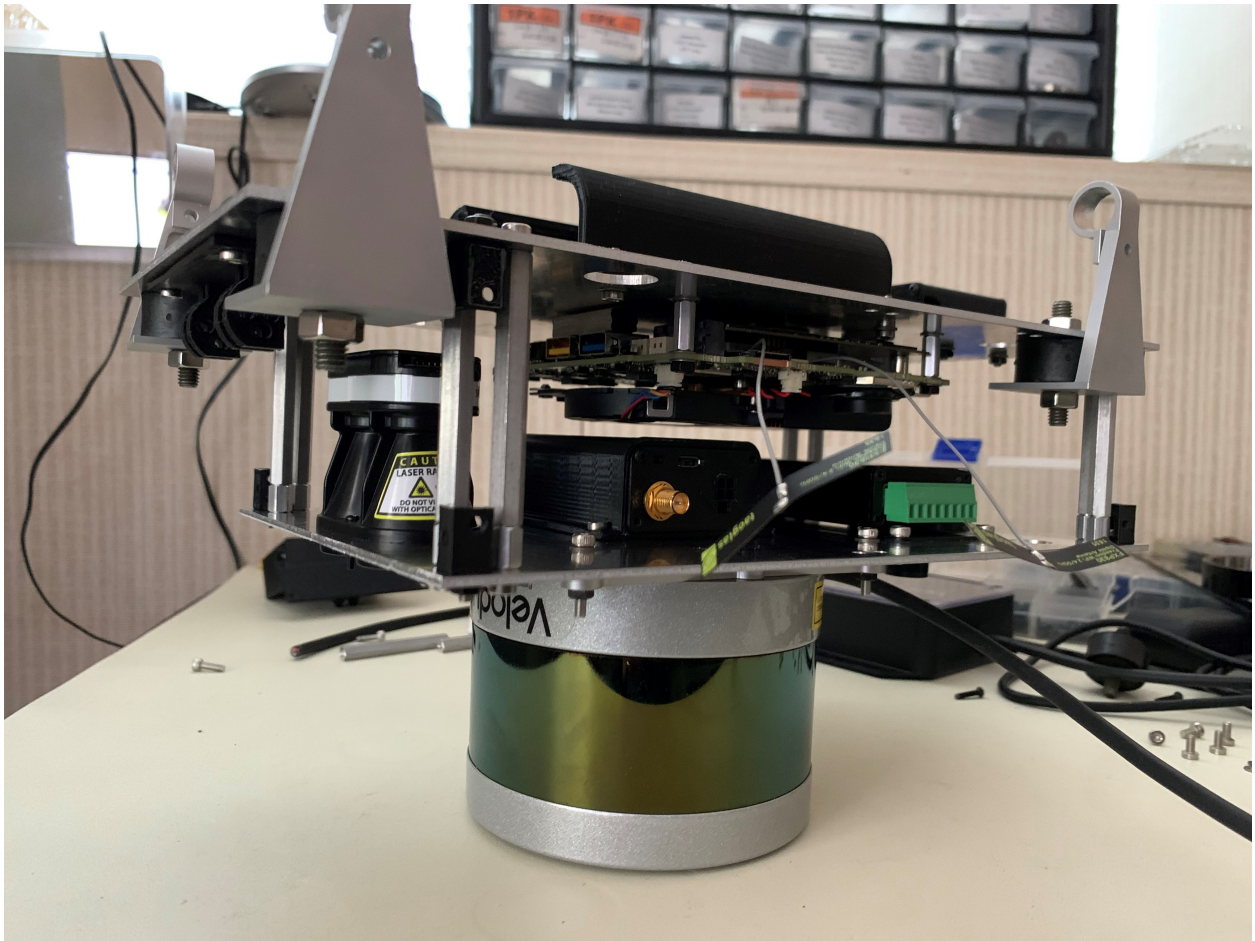


Figure 9: First assembly of the Gen 3 payload. All of the components are shown mounted except for the smart battery and visible/thermal camera.

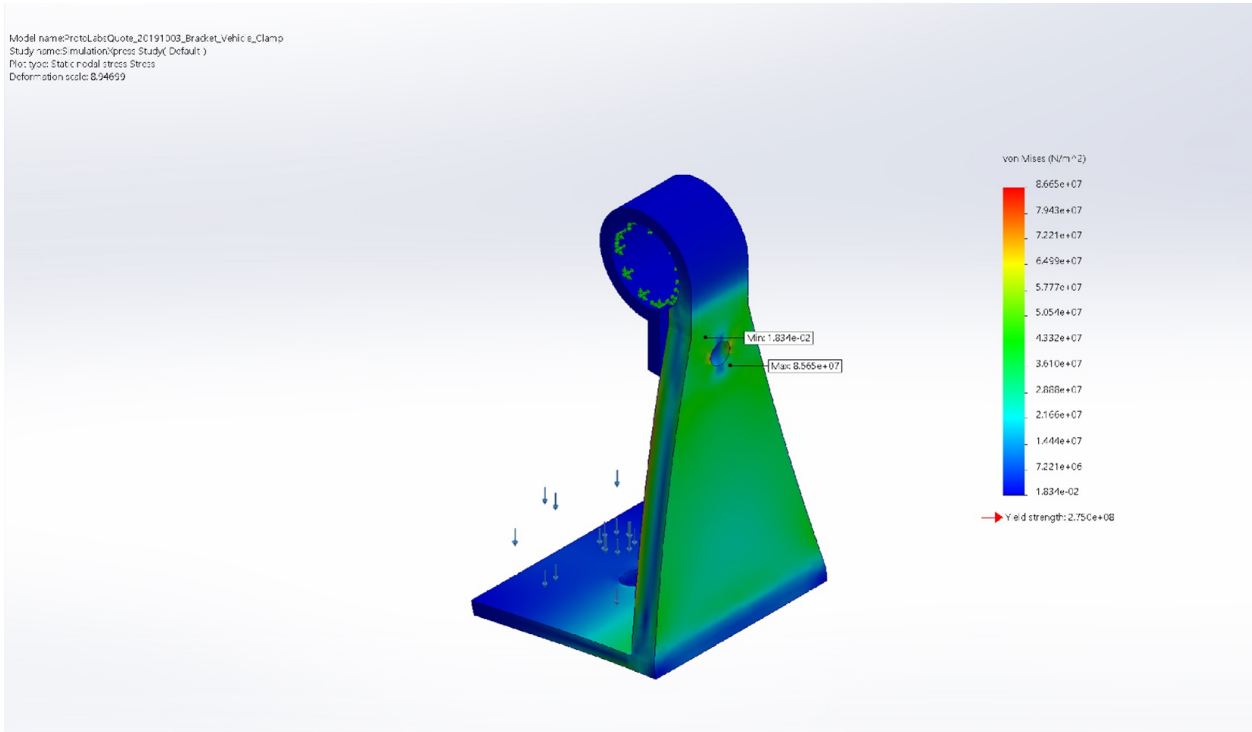


Figure 10: Mounting rail clamp von Mises stress profile conducted in Solidworks. The part is fixed at the top clamp where the part fixes onto the payload rack. The load is applied downwards on the surface where the vibration damping sandwich mount sits. 67.38 N is applied at the load point. The minimum factor of safety is 3.17.

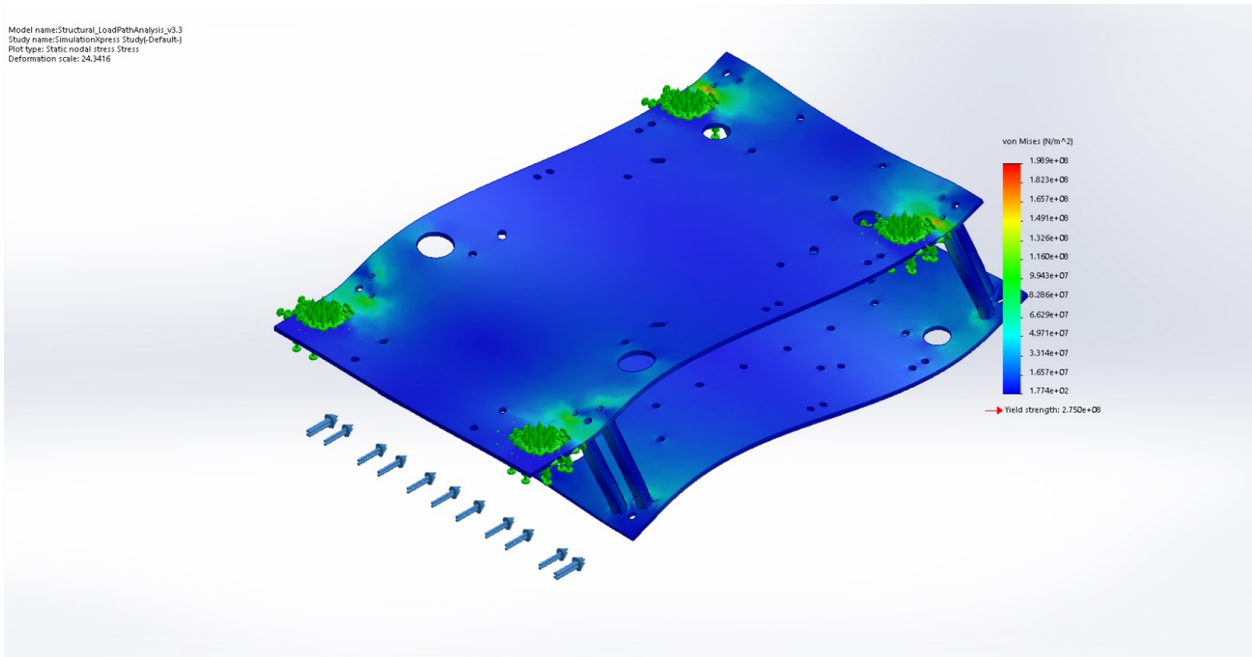


Figure 11: Gen 3 payload structural frame von Mises stress profile conducted in Solidworks. The structural frame consists of the battery and bottom plate connect by aluminum hex standoffs and is fixed at the vibration damper sandwich mounts. Assumes a max payload of 5500 g in a 5 G maneuver for 269.5 N applied to the front face of the bottom plate for a worst case scenario. The minimum factor of safety is 1.38.

IV. Simulation

Not only does Reflection serve as the processing architecture for the autonomy modules, but it also enables physics-based testing and simulation.⁶ Onboard decision-making,⁸ V2V communication,⁹ path planning,^{7,9} and wind modeling¹ have already been tested within Reflection simulation and hardware in the loop. Future simulations will be conducted to test several functions before actual flight tests, including UTM airspace allocation, multiple vehicle deconfliction, and wildfire modeling, mapping, detection, and tracking.

V. Flight Tests

As previously mentioned, a previous iteration of the Gen 2.1 payload has been flown at NASA Ames over the years.⁵ However, that older payload connected to a Pixhawk autopilot to control a DJI S1000. The open source Pixhawk easily integrated with the onboard computer's flight control commands. The DJI M600 Pro flies the DJI flight stack through the A3 Pro, making flight control through a payload more complex. The following tests served as steps towards payload integrated flight on the M600 Pro.

A. Gen 2.1 Payload – LIDAR Drive Test

The 360° LIDAR was used to gather point cloud data of NASA Ames Research Center. To do this, the M600 Pro with the mounted Gen 2.1 payload was strapped to the roof the car shown in Figure 12. The payload was powered to collect and store LIDAR point cloud data on the onboard computer in the form of rosbag files for post-processing. The aircraft was also powered on so that the DJI A3 Pro autopilot was able to collect telemetry data during the drive. All program execution was done via ssh from a laptop being operated in a vehicle following the aircraft.



Figure 12: Drive test rig where the M600 Pro was secured to a car to test LIDAR point cloud collection with the Gen 2.1 payload.

Figure 13 shows the path driven by the car carrying the M600 Pro. This path was chosen to be the trajectory the aircraft takes for the future flight tests at Ames. The point cloud data shown in Figure 14 is being used to create an a priori map of Ames that can be loaded onto the onboard computer during pre-flight to plan a global path between buildings and avoiding trees and powerlines. The a priori map is information a sUAS in UTM would have when generating its flight plan. However, it should be expected that there could be obstacles during flight that were not known in the a priori map. Thus, the sUAS should have means to

C. Gen 2.1 Payload – Integration Flight Test

Integration between the onboard computer running Reflection and the A3 Pro autopilot was demonstrated in flight. The onboard computer integrated the DJI onboard SDK into Reflection to enable outer-loop control of the aircraft. The M600 Pro was manually commanded to take-off via RC. Once hovering, the onboard computer sent joystick velocity commands to the A3 Pro autopilot to fly along a straight path. Although this is not autonomous flight, outer-loop control is a powerful tool that enables platform-agnostic autonomy capabilities. By not touching the inner-loop flight controller, the Reflection autonomy architecture should be compatible with any aircraft where velocity commands are accepted as inputs.

D. Future Flight Test

Future flight tests include testing in-flight V2V communication, leveraging the UTM infrastructure to allocate airspace with the M600 Pro, global path planning in an a priori map, local path planning around detected objects, and fire detection. All of these capabilities contribute towards an autonomous sUAS and can be tested individually before completely integrating with each other. While the Gen 2.1 payload may be capable of semi-autonomous flight, it serves as a stepping stone for the Gen 3 payload to enable autonomy.

VI. Conclusion

We have shown two payloads that work towards autonomous sUAS flight in UTM TCL4+ and STEReO. The Gen 2.1 payload has demonstrated LIDAR SLAM and outer-loop control over the DJI A3 autopilot by sending Reflection joystick velocity commands. The outer-loop control can be combined with an onboard path planner that calculates velocity commands to waypoints. SLAM information from the LIDAR can then be used to update the waypoints based on obstacles along the current flight path. In addition to what is already on the Gen 2.1 payload, the Gen 3 payload has a dual visible light and thermal camera for ground risk mitigation and fire detection, a downward-facing monocular camera for safe landing detection, a V2V radio modem for cooperative sense and avoid, a laser range finder altimeter for accurate AGL altitude, and a smart battery for more efficient path planning. The V2V modem and dual camera have already been tested in hardware in the loop simulation and the other components will be tested before integrating with the Gen 3 payload. At the time of this paper, the Gen 2.1 payload has demonstrated flight readiness and the Gen 3 payload is in development stage. Future Gen 2.1 flight tests include leveraging the UTM infrastructure to generate a deconflicted flight plan and adding the dual visible light and thermal camera for fire detection and tracking. After fully integrating the Gen 3 payload components, flight tests will be conducted to test individual autonomy capabilities, such as V2V communication and path planning.

Acknowledgments

The authors would like to thank our colleagues in the NASA SAFE50, UTM, and STEReO projects for their collaboration and insight.

References

- ¹Krishnakumar, K. S., Kopardekar, P. H., Ippolito, C. A., Melton, J., Stepanyan, V., Sankararaman, S., and Nikaido, B., “Safe Autonomous Flight Environment (SAFE50) for the Notional Last “50 ft” of Operation of “55 lb” Class of UAS,” *AIAA Information Systems-AIAA Infotech@ Aerospace*, 2017, p. 0445.
- ²Kopardekar, P. H., “Unmanned aerial system (UAS) traffic management (UTM): Enabling low-altitude airspace and UAS operations,” 2014.
- ³Rios, J. and Johnson, M., “Unmanned Aircraft Systems Traffic Management (UTM) Concepts and Architecture Overview, v2.0,” 2020.
- ⁴Mercer, J. and Glaab, L., “Scalable Traffic Management for Emergency Response Operations (STEReO),” 2019.
- ⁵Hening, S., Ippolito, C. A., Krishnakumar, K. S., Stepanyan, V., and Teodorescu, M., “3D LiDAR SLAM Integration with GPS/INS for UAVs in Urban GPS-Degraded Environments,” *AIAA Information Systems-AIAA Infotech@ Aerospace*, 2017, p. 0448.
- ⁶Ippolito, C. A., Hening, S., Sankararaman, S., and Stepanyan, V., “A modeling, simulation and control framework for small unmanned multicopter platforms in urban environments,” *2018 AIAA Modeling and Simulation Technologies Conference*, 2018, p. 1915.

⁷Chakrabarty, A. and Ippolito, C. A., “Autonomous flight for Multi-copters flying in UTM-TCL4+ sharing common airspace,” *AIAA Scitech 2020 Forum*, 2020, p. 0881.

⁸Baculi, J. E. and Ippolito, C. A., “Onboard Decision-Making for Nominal and Contingency sUAS Flight,” *AIAA Scitech 2019 Forum*, 2019, p. 1457.

⁹Chakrabarty, A., Ippolito, C. A., Baculi, J., Krishnakumar, K. S., and Hening, S., “Vehicle to Vehicle (V2V) communication for Collision avoidance for Multi-copters flying in UTM-TCL4,” *AIAA Scitech 2019 Forum*, 2019, p. 0690.

¹⁰Chakrabarty, A., Stepanyan, V., Krishnakumar, K. S., and Ippolito, C. A., “Real-Time Path Planning for Multi-copters flying in UTM-TCL4,” *AIAA Scitech 2019 Forum*, 2019, p. 0958.

¹¹Ippolito, C. A., “Dynamic Ground Risk Mitigation for Autonomous Small UAS in Urban Environments,” *AIAA Scitech 2019 Forum*, 2019, p. 0961.

¹²Matrice, D., “600 Pro,” 2019.